

Earthquake Frequency and Ground Motion Specification for the SNR-300 Risk Oriented Analysis

L. Ahorner

Erdbebenstation, Universität Köln, Vincenz-Pallotti-Str. 26, D-5050 Bergisch-Gladbach 1, Germany

W. Rosenhauer

INTERATOM GmbH, Postfach, D-5060 Bergisch-Gladbach 1, Germany

Abstract

Site specific engineering parameters are determined as required for the calculation of intensity attached fragility curves, together with the intensity probability distribution.

An existing probabilistic seismicity model of the site environment is evaluated, applying the latest methodological state, e. g. a magnitude frequency curve derived from a generalized Gumbel distribution and Monte-Carlo procedures including attenuation law uncertainties. Macro-seismic load collectives exhibit the most probable ranges of focal parameters consistent with a given site intensity. Response spectra are consequently derived avoiding the usual detour via peak acceleration and its poor correlation to intensity.

The results demonstrate that the SSE of the plant is conservative and that safe and reasonable seismic load definitions are available, due to the past 10 years' seismological research.

1 Introduction

Protection against earthquakes has been an important and expensive subject for construction and licensing of the fast breeder prototype reactor SNR-300. The site near Kalkar is situated in the Lower Rhine embayment about 100 km north-west of Cologne, Federal Republic of Germany.

Operating base and safe shutdown earthquakes for the plant were fixed in 1972. Seismological knowledge has much improved due to the past 10 years' research. Probabilistic seismic site analysis has been developed in order to obtain reliable estimates of the specific seismic hazard and to establish seismic load assumptions for nuclear plants in a more rational and transparent manner vice versa. These methods make possible to supply basic data for risk analyses, too, beyond their original target.

The aim of the SNR-300 Risk Oriented Analysis / 1 / was a comparison with the results of the German Risk Study for LWR plants / 2 /. The assessment of earthquake induced risk was an important subtask in both investigations. For SNR-300 ground motions had to be considered down to a frequency of about $10^{-8}/a$, which was not necessary for the PWR, because of the very small probability of breeder core disruptive accidents caused by internal events.

The newly determined seismic loads represent (as an intended by-product) a check of the SNR-300 design earthquakes and allow conclusions concerning the future trends.

2 Seismic Source and Effect Model

The local and regional geotectonic and seismological information, which is the decisive contingent to a seismic hazard analysis, has recently been reviewed by Ahorner / 3 /.

Kalkar is situated outside the Rhenish and Belgian earthquake regions, for which sufficient magnitude data gained by reinterpretation of events in the past centuries have been compiled by Ahorner / 3 /, / 8 /.

Three of the focal zones identified for the Lower Rhine area by the authors in / 4 / are relevant for the site. New magnitude frequency relations for each zone (see fig. 1 as an example) have been determined from magnitude extremes.

They have been derived using a generalized Gumbel distribution for extreme values of a possibly not unbounded variable (details see Rosenhauer / 5 /), and are characterized by mean value m and standard variation σ of the extremes, and by a parameter $\tau \geq 0$ simply connected to the skewness (third moment). The well known Gutenberg and Richter straight line is the limiting case $\tau \rightarrow 0$ ($M_{\max} \rightarrow \infty$), the original Gumbel distribution. The main advantage of this approach is that the essential part of the curve is almost independent of τ and the upper magnitude bound M_{\max} , parameters which are therefore not required with high accuracy if $\tau > 0$ ($M_{\max} < \infty$) is found valid.

Magnitude dependent probability distributions for the focal depth, which is between 1 km and 25 km, complete the source model.

The parameter governing the ground motion definition for sites in Central Europe is the macroseismic intensity I (MSK-scale). Extensive local information is available via intensity data, whereas e. g. peak accelerations $a_{\max} \geq 0.05$ g were measured only twice (in the Swabian Jura) for the Rhine area and adjacent regions.

The use of an adopted mean curve for the attenuation of a_{\max} with focal distance led to huge uncertainties, consequently, which were difficult to discuss, / 4 / and Rosenhauer / 6 /. The attenuation of I with hypocentral distance R was verified (see / 3 /), on the other hand, using local data to be

$$I(R,M) = 1.5 M - a_1 - a_2 \log_{10} (R/10 \text{ km}) - a_3 (R/\text{km} - 10) \quad (1)$$

$$a_1 = 1.0 \quad (0.5 \dots 1.5)$$

$$a_2 = 3.0 \quad (2.5 \dots 4.0)$$

$$a_3 = 0.003 \quad (0.001 \dots 0.01)$$

with uncertainty ranges around the mean curve specifying the possible deviation a single event might show.

The intensity is not directly applicable for design purposes and quantitative risk analyses, though it provides a classification of the earthquake scenario as a basis of qualitative discussions of consequences, for which the high frequency response a_{\max} is particularly unfit. Severe additional drawbacks concerning the use of a_{\max} and standardized response spectra have been realized during the last years.

Satisfactory correlations between a_{\max} and I, for instance, are lacking even for more active regions of the world, too. Derivations of spectra are under development, therefore, which avoid this detour. A first version of such methods as applied to Kalkar is presented in section 4, whereas the next section sketches a general starting-point available for these approaches.

3 Macroseismic Load Collectives

The seismic source and effect description is a probabilistic model, corresponding to the stochastic nature of future earthquake occurrence. Site specific investigations are favourably performed by Monte-Carlo simulation techniques, / 5 /.

Artificial earthquake catalogues are produced by this method. Simple counting yields the probabilities of interesting site intensities, e. g. due to different hypocentral focal distances, fig. 2. These results cover, above all, the uncertainties caused by individual attenuation laws (/ 5 /, / 6 /), scattering according to eq. (1), an effect which was found difficult to include by other methods.

The prevailing aim of the simulation has been, however, to create representative sets of focal events (called macroseismic load collectives) belonging to prescribed site effects. About 50 earthquakes for each of the site intensity intervals $6 \pm 1/4$, $6 \frac{1}{2} \pm 1/4$, $7 \pm 1/4$, $7 \frac{1}{2} \pm 1/4$, $8 \pm 1/4$ and $> 8 \frac{1}{4}$ were simulated. They allow to determine the expected intensity dependent magnitude ranges, fig. 3 for $R = (25 \pm 10)$ km, mainly contributing to the seismic hazard (fig. 2).

Fig. 3 confirms that a shock with local magnitude $M_L \approx 6$ in hypocentral distance $R \approx 25$ km is a safe choice for an event representing $I = VII$, the intensity of the SSE of the SNR-300 (Ahorner / 7 /).

4 Engineering Ground Motion Parameters

The identification of the appropriate focal parameters opens the way to site specific spectra attached to intensity, derived from records for comparable soil and subsoil conditions as an additional limitation.

Single response spectra were computed correspondingly from twelve horizontal acceleration time histories of three Friaul 1976 earthquakes with magnitudes between $M_L = 5.9$ and 6.2 , recorded at two stations (Forgaria-Cornino and Buia) in the near-field, $R = (16 \pm 3)$ km.

Mean spectra were calculated without the usual normalization at high frequencies ($/ 3 /$, $/ 7 /$), thus disclosing the true variance for the whole frequency range. No peak acceleration renormalization had to be performed as a consequence. Adaption to the correct hypocentral distance and smoothing led to the model spectrum and its standard deviation for a single horizontal component shown in fig. 4.

A rough upper bound for the horizontal vector peak acceleration b_0 is in astonishing agreement with 120 cm/s^2 , the SSE value of the SNR-300,

$$b_0 < \sqrt{2} a_{\max} = \sqrt{2} \cdot 0.83 \text{ m/s}^2 = 1.17 \text{ m/s}^2 \quad (2)$$

A spectrum formed analogously from a_r of fig. 4 for all frequencies is not unsimilar to the SNR-300 SSE design spectrum as well.

Earthquakes stronger and weaker than the SSE had to be considered in the risk analyses, too, fig. 2. A variation of a_r with a factor

$$F = 10^{0.3 (I-7)}, \text{ VI} \leq I \text{ (MSK)} \leq \text{VIII} \quad (3)$$

was proposed for this purpose.

An important parameter for nonlinear dynamic calculations is the duration t_0 of the strong motion phase (fig. 5), which was conveniently defined by first and last exceedance of $a_{\max}/3$ of each time history. A good fit was reached with a uniform distribution of $\log t_0$ between $t_0 = 1.6$ s and 8.5 s, fig. 5.

5 Conclusions

The specification of realistic ground motions exceeding the events observed at nuclear sites in the past is required for the definition of design loads because of safety reasons, and for risk analyses. The inevitable extrapolations, conservative assumptions, uncertainties etc. are best treated in a valuing and transparent manner by a probabilistic model, representing all available geotectonic and seismological knowledge.

Results have been presented filling the gap between the original seismological description of site effects by the macroseismic intensity and engineering parameters, avoiding the use of peak acceleration with its inherent deficiencies.

The SSE chosen for the design of the SNR-300 was checked to be conservative, concerning its probability of $4 \cdot 10^{-6}/a$ as well as with respect to the design response spectrum. Safe and reasonable seismic loads will result from an intended adaption of existing rules covering today's methods and experience of seismology.

References

- / 1 / Risikoorientierte Analyse zum SNR-300, Abschlußbericht zum BMFT-Förderungsvorhaben RS 510, Gesellschaft für Reaktorsicherheit (GRS), April 1982
- and contributions of D. Hosser and K. Köberlein to this conference
- / 2 / German Risk Study - Main Report, A Study of the Risk due to Accidents in Nuclear Power Plants by the Gesellschaft für Reaktorsicherheit (GRS), EPRI NP-1804-SR, April 1981
- / 3 / Ahorner, L., Seismicity and Neotectonic Structural Activity of the Rhine Graben System in Central Europe, in "Seismicity and Seismic Risk in the North Sea Offshore Area", edited by A. R. Ritsema and A. Gürpınar, Reidel, Dordrecht, The Netherlands (1982)
- / 4 / Ahorner, L., Rosenhauer, W., "Probability Distribution of Earthquake Acceleration with Applications to Sites in the Northern Rhine Area, Central Europe", J. Geophys. 41, 581 - 594 (1975)
- / 5 / Rosenhauer, W., Methodological Aspects Encountered in the Lower Rhine Area Seismic Hazard Analysis, l. c. in / 3 / (1982)

- / 6 / Rosenhauer, W., The Role of Attenuation Law Uncertainties in Probabilistic Seismic Hazard Analyses, Proceedings CSNI Specialist Meeting on "Probabilistic Methods in Seismic Risk Assessment for Nuclear Power Plants", Lisbon, Portugal, 30.09. - 03.10.80
- / 7 / Ahorner, L., "Realistische Abschätzung der Erdbebenlastannahmen für den Standort SNR-300 bei Kalkar am Niederrhein nach dem derzeitigen seismologischen Kenntnisstand", Bericht im Auftrag von König und Heunisch, Bensberg, 20. März 1982
- / 8 / Ahorner, L., "Present-day stress field and seismotectonic block movements along major fault zones in Central Europe", Tectonophysics 29, 233 - 249 (1975)

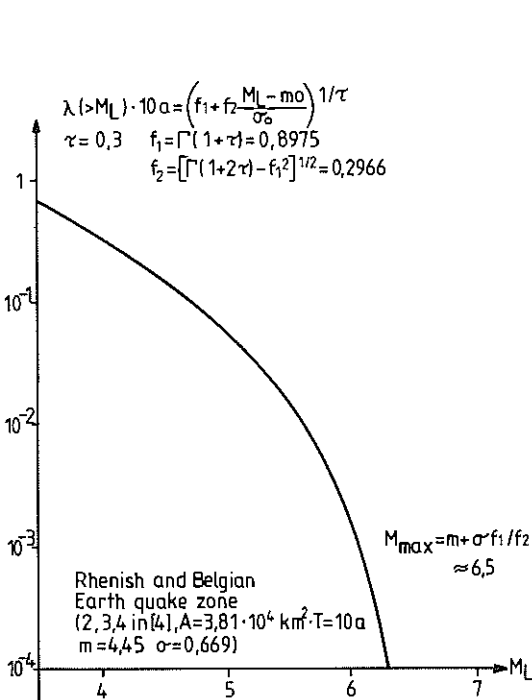


Fig. 1: Magnitude frequency curve derived from the generalized Gumbel distribution, normalized to $A_0 = 10^4 \text{ km}^2$, $T_0 = 10 \text{ a}$

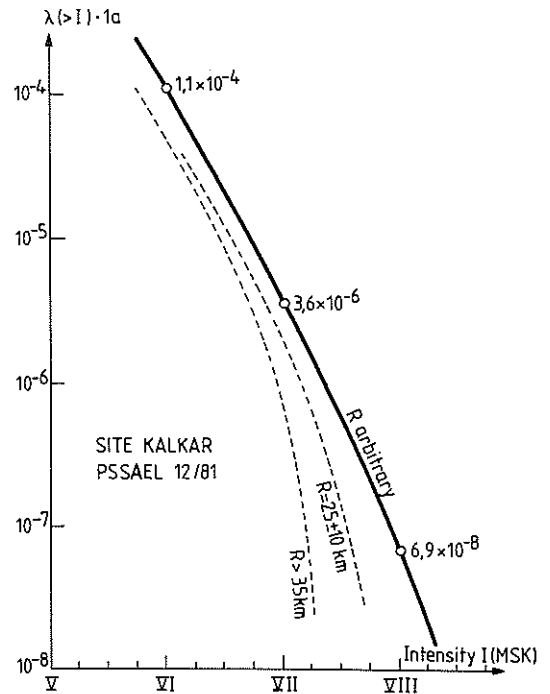


Fig. 2: Frequency of earthquake intensity for SNR-300

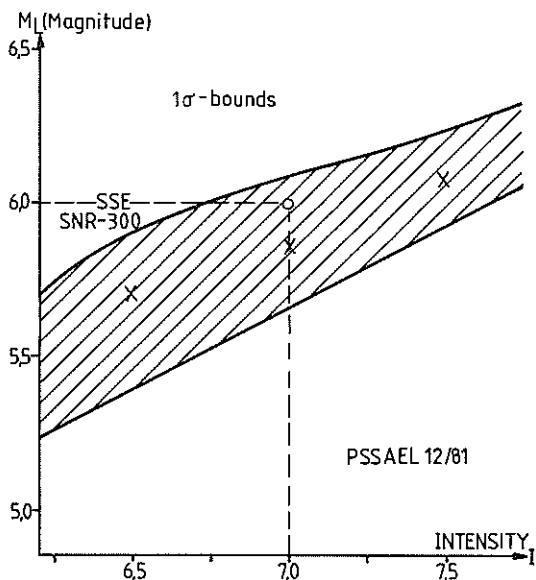


Fig. 3: Magnitude ranges for intensities $I \pm 1/4$, hypocentral distances $R = (25 \pm 10)$ km, site Kalkar

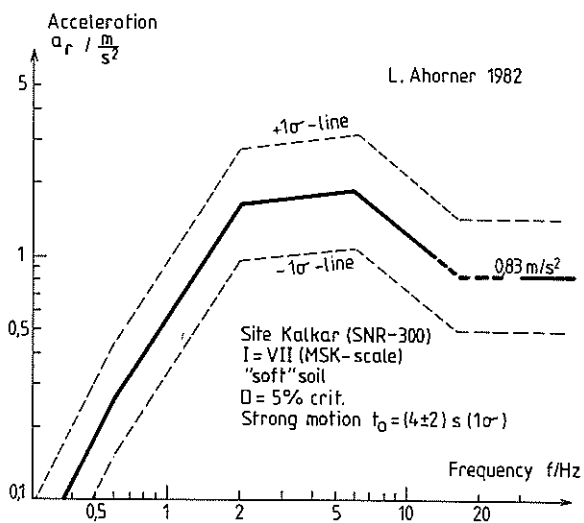


Fig. 4: Free field model response spectrum and its standard variation for a horizontal component

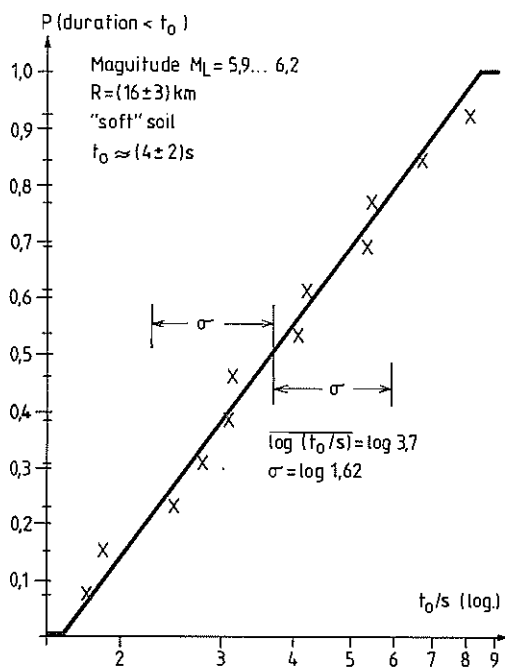


Fig. 5: Empirical distribution of duration t_0 between first and last exceedance of $a_{max}/3$